

Rational Development of a Polysaccharide–Protein-Conjugated Nanoparticle Vaccine Against SARS-CoV-2 Variants and *Streptococcus pneumoniae*

Yongqiang Deng, Jing Li, Chunyun Sun, Hang Chi, Dan Luo, Rui Wang, Hongying Qiu, Yanjing Zhang, Mei Wu, Xiao Zhang, Xun Huang, Liangzhi Xie,* and Chengfeng Qin*

The ongoing COVID-19 pandemic caused by SARS-CoV-2 has led to millions of deaths worldwide. *Streptococcus pneumoniae* (*S. pneumoniae*) remains a major cause of mortality in underdeveloped countries. A vaccine that prevents both SARS-CoV-2 and *S. pneumoniae* infection represents a long-sought “magic bullet”. Herein, a nanoparticle vaccine, termed SCTV01B, is rationally developed by using the capsular polysaccharide of *S. pneumoniae* serotype 14 (PPS14) as the backbone to conjugate with the recombinant receptor-binding domain (RBD) of the SARS-CoV-2 spike protein. The final formulation of conjugated nanoparticles in the network structure exhibits high thermal stability. Immunization with SCTV01B induces potent humoral and Type 1/Type 2 T helper cell (Th1/Th2) cellular immune responses in mice, rats, and rhesus macaques. In particular, SCTV01B-immunized serum not only broadly cross-neutralizes all SARS-CoV-2 variants of concern (VOCs), including the most recent Omicron variant, but also shows high opsonophagocytic activity (OPA) against *S. pneumoniae* serotype 14. Finally, SCTV01B vaccination confers protection against challenges with the SARS-CoV-2 mouse-adapted strain and the original strain in established murine models. Collectively, these promising preclinical results support further clinical evaluation of SCTV01B, highlighting the potency of polysaccharide-RBD-conjugated nanoparticle vaccine platforms for the development of vaccines for COVID-19 and other infectious diseases.

1. Introduction

Coronavirus disease 2019 (COVID-19), caused by infection with severe acute respiratory syndrome coronavirus 2 (SARS-CoV-2), emerged in late 2019, causing a global pandemic that has lasted for more than 2 years. Under the cooperative efforts of the science community and the vaccine industry, several types of COVID-19 vaccines, including inactivated vaccines,^[1] adenovirus-based vaccines,^[2] mRNA vaccines,^[3] and recombinant protein vaccines,^[4] have been approved and used for vaccination worldwide. In general, recombinant protein vaccines have typically shown lower immunogenicity than virus and mRNA vaccines and hence require the usage of various adjuvants.


The trimeric spike protein of SARS-CoV-2 contains the receptor-binding domain (RBD) that binds to the human angiotensin-converting enzyme 2 (ACE2) receptor on the membrane of epithelial cells. Blocking the binding between RBD and ACE2 can effectively inhibit and prevent viral infection.^[5] A high titer of serum antibody against the RBD protein can be

detected in COVID-19 patients 10 days after symptom onset.^[6] In SARS-CoV-2-infected patients, significant humoral and T-cell responses to RBD are detected. Thus, both the RBD and spike protein are key targets as COVID-19 vaccine antigens. Importantly, RBD can be easily produced at a high yield with classic CHO cell-based antibody production platform technology and existing commercial facilities. Due to the small molecule size of RBD, various efforts have been made to enhance its immunogenicity. Some nanoparticle COVID-19 vaccines designed as RBD dimers^[7] have been shown to elicit more potent immune responses than RBD monomers. Other strategies have also been used for the development of surface-displayed SARS-CoV-2 RBD protein vaccine candidates, including virus-like particle (VLP) platforms,^[8] liposomes,^[9] ferritin nanocages,^[10] *Lactobacillus plantarum*,^[11] and *Saccharomyces cerevisiae*.^[12] These studies confirm that particulate presentation strategies for the RBD immunogen promote RBD uptake into antigen-presenting cells, thus inducing stronger antibody responses.

Y. Deng, H. Chi, D. Luo, H. Qiu, M. Wu, X. Huang, C. Qin
Department of Virology
State Key Laboratory of Pathogen and Biosecurity
Beijing Institute of Microbiology and Epidemiology
AMMS
Beijing 100071, P. R. China
E-mail: qincf@bmi.ac.cn, chengfeng_qin@126.com

J. Li, C. Sun, R. Wang, Y. Zhang, X. Zhang, L. Xie
Beijing Protein and Antibody R&D Engineering Center
Sinocelltech Ltd.
Beijing 100176, P. R. China
E-mail: liangzhi@yahoo.com

C. Qin
Research Unit of Discovery and Tracing of Natural Focus Diseases
Chinese Academy of Medical Sciences
Beijing 100071, P. R. China

 The ORCID identification number(s) for the author(s) of this article can be found under <https://doi.org/10.1002/adma.202200443>.

DOI: 10.1002/adma.202200443

Polysaccharide vaccines against bacterial infections have been well developed. In particular, the conjugation of polysaccharides to protein carriers has been used to improve immunogenicity, and several polysaccharide–protein conjugate vaccines are now available to prevent *Haemophilus influenzae* type B (Hib), *Neissera meningitides*, and *S. pneumoniae* infections.^[13] At present, tetanus or diphtheria toxoid proteins are the most common carrier proteins used; few viral proteins have been used as carriers.^[14] Interestingly, polysaccharides were reported as antigen-loaded nanocarriers in HIV peptide vaccines.^[15] In particular, the capsular polysaccharide of *S. pneumoniae* serotype type 14 (PPS14), which is an acidic polysaccharide composed of repeating linear and branched oligosaccharide units, can mediate conjugated antigen cross-interaction with B-cell receptors (BCRs), C-type lectin receptors (CLRs), and mannose receptors (MRs) on antigen-presenting cells (APCs) such as dendritic cells (DCs) and then promote antigen internalization, processing, and presentation.^[16] The presence of these secondary signals is supposed to enhance antigenicity and induce an antigen-specific T-cell response, such as in *meningococcal meningitis*. The serogroup C polysaccharide is not immunogenic in children younger than 2 years of age, while a three-dose regimen of *meningococcal* glycoconjugate vaccines elicits specific anti-polysaccharide antibody titers in infants and young children.^[17] Otherwise, *S. pneumoniae* serotype 14 is one of the most common types worldwide, and hence, it is one of the most important serotypes included in all pneumococcal conjugate vaccines.

At present, no polysaccharide-conjugated vaccine has been developed to prevent SARS-CoV-2 or other viral diseases. In this study, we designed and prepared a novel nanoparticle vaccine by chemically conjugating recombinant SARS-CoV-2 RBD and PPS14. Preclinical studies have demonstrated that SCTV01B vaccination induced potent and broad neutralizing antibodies and cellular immune responses against SARS-CoV-2 in mice, rats, and nonhuman primates, as well as high OPA against *S. pneumoniae* serotype 14. Therefore, SCTV01B represents a promising vaccine candidate for preventing both COVID-19 and *S. pneumoniae* infection-related pneumonia.

2. Results

2.1. Design, Preparation, and Characterization of SCTV01B

To prepare the polysaccharide–protein conjugated nanoparticle vaccine, PPS14 was used as the antigen-backbone nanocarrier to couple with the recombinant RBD protein of SARS-CoV-2 (Figure 1a). Recombinant RBD (319–531 aa) was expressed in Chinese hamster ovary (CHO) cells, and the molecular size of recombinant glycosylated RBD protein ranged from 28 to 32 kD with a band purity >99.9% (Figure 1b). The BLI results showed that recombinant RBD protein could specifically bind to its receptor ACE2 with an affinity of 58×10^{-9} M (Figure 1c). Meanwhile, PPS14 was separated from *S. pneumoniae* lysates by centrifugation, ultrafiltration, acid precipitation, and subsequent purification with chromatography and ultrafiltration (Figure 1a). The nuclear

magnetic resonance (NMR) spectrum of three lots of PPS14 showed identical signal peaks at the corresponding areas (Figure 1d). Then, the chemical conjugation process of PPS14 and SARS-CoV-2 RBD protein was performed at an average ratio of 1:13 using the reductive amination method (Figure 1a). The developed RBD/PPS14 conjugate had a protein/polysaccharide mass ratio of 0.7:1, as detected by ultraviolet (UV) and phenol–sulfuric acid (PHS) methods. Quantitative analysis of the SEC-HPLC results showed that the target component of conjugated SCTV01B was >92% (Figure S1, Supporting Information). Transmission electron microscopy (TEM) analysis indicated that the conjugated SCTV01B was composed of nanoparticles with diameters ranging from 8 to 23 nm (Figure 1e). Importantly, the differential scanning fluorimetry (DSF) results showed that SCTV01B exhibited high thermal stability based on T_m and T_{agg} and polymerized until 74.0 °C (Figure 1f). Taken together, these results showed that recombinant SARS-CoV-2 RBD was successfully conjugated with PPS14, and the resulting SCTV01B nanoparticles were quite thermally stable.

2.2. SCTV01B Induced Robust Humoral and T-Cell Responses in Mice and Rats

To evaluate the immunogenicity of SCTV01B, adult hACE2 mice^[18] and aged BALB/c mice^[19] were used for intramuscular immunization with SCTV01B combined with adjuvant or an equal volume of adjuvant alone as a negative control three times over an interval of 21 days (Figure 2a,f). The results indicated that both RBD-specific IgG and pseudovirus (PSV)-neutralizing antibodies in two mice were elevated in a dose-dependent manner after the second injection. RBD-specific IgG titers after vaccination with SCTV01B in hACE2 mice at 1, 3, and 10 µg using the prime/boost regimen reached 1/67806, 1/128000, and 1/215269 (Figure 2b), and NT₅₀ titers reached 1/2985, 1/26262, and 1/17614 (Figure 2c) at day 14 postboosting, respectively. A further boost with a third dose increased anti-RBD IgG titers and NT₅₀ titers by an average of four- to fivefold in all dose groups (Figure 2b,c; Table S1, Supporting Information), and the titers could be maintained for at least 7 weeks without obvious decreases (Figure S2a,b, Supporting Information). Similarly high levels of immune responses were also observed in the aged BALB/c mice after immunization with 1 and 3 µg of SCTV01B with three injections, with the highest IgG titer of >10^{4.9} and NT₅₀ titer of 10^{4.0} (Figure 2g,h; Table S2, Supporting Information). Furthermore, strong RBD-specific IgG and NT₅₀ titers were also observed in adult BALB/c mice vaccinated with 1 and 10 µg of SCTV01B (Figure S3a,b, Supporting Information) and in SD rats vaccinated with 20 or 60 µg of SCTV01B (Figure S3c,d, Supporting Information).

RBD-specific IFN- γ (Th1, Type 1 T helper cell) or IL-4 (Th2, Type 2 T helper cell)-positive splenic spot-forming cells (SFCs) were detected by ELISpot assays. The results indicated that strong cellular T-cell responses were observed in hACE2 mice (Figure 2d,e; Table S3, Supporting Information) and aged BALB/c mice (Figure 2i,j; Table S4, Supporting Information) after two doses of SCTV01B. Meanwhile, obviously increased

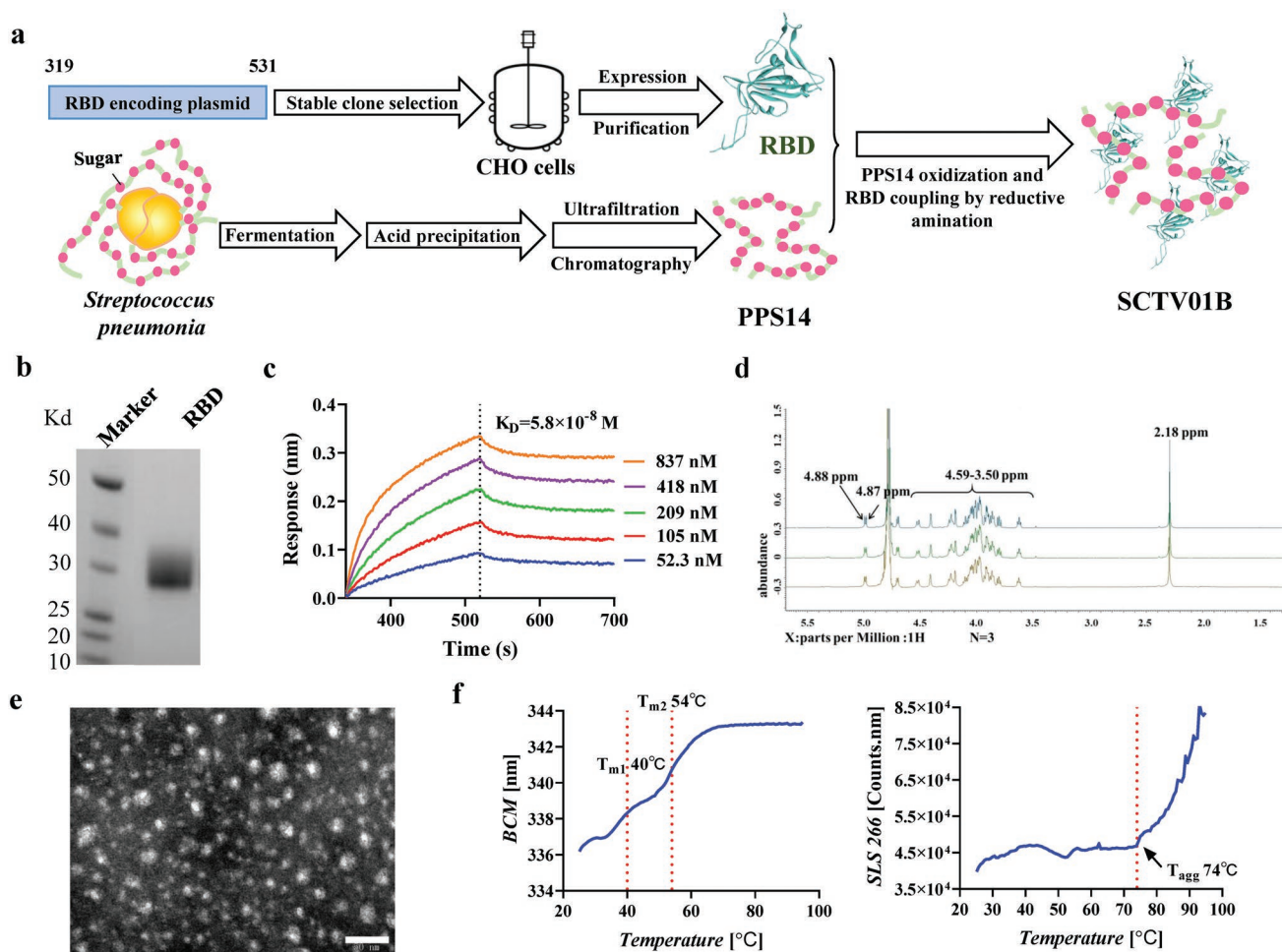


Figure 1. Design and Characterization of SCTV01B. a) Experimental design and workflow for the preparation of SCTV01B. The SARS-CoV-2 RBD was expressed in CHO cells. PPS14 was produced from *S. pneumoniae* by the acid precipitation method and conjugated with RBD utilizing the reductive amination method. b) Identifying the molecular weight of RBD by NuPAGE. c) Binding affinity of RBD to its ACE2 receptor using the BLI method. d) NMR spectrum of PPS14 saccharide residue components and structure analysis (3 lots): containing glucose and *N*-acetyl glucose groups with peaks at 4.88 ppm (parts per million) and galactose groups with peaks at 4.87 ppm. Peaks in the 4.59–3.50 ppm region were attributed to ring protons, and peaks in the 2.18 ppm region were attributed to *N*-acetyl groups. e) Transmission electron microscopy of SCTV01B showed nanoparticles with heterogeneous diameters (scale bar = 50 nm). f) The thermostability of SCTV01B was characterized by T_m and T_{agg} .

IFN- γ^+ CD4 $^+$ T and CD8 $^+$ T cells in the total splenic population detected by ICS assay were observed in SCTV01B-vaccinated hACE2 mice and aged BALB/c mice (Figure S4a,c,e,g, Supporting Information). The activated RBD-specific CD40L $^+$ (CD154 $^+$) T-cell responses that helped B cells with efficient isotype switching^[20] to secrete the high-affinity RBD-specific neutralizing antibodies are shown in Figure S4b,d,f,h (Supporting Information).

2.3. SCTV01B Induced Potent Humoral and Th1-Biased Cellular Immune Responses in Mice

To evaluate the contribution of PPS14 to SCTV01B-induced immunity, we compared the immune responses induced by SCTV01B or unconjugated RBD antigen with the same adjuvant in adult BALB/c mice. The results showed that SCTV01B induced a 23-fold higher IgG titer and a 5.5-fold higher NT₅₀

titer than the unconjugated RBD at day 21 after the priming dose, indicating that the PPS14-conjugated nanoparticle antigen was much more immunogenic and induced a more rapid immune response. After two weeks of the boost dose, a time when the vaccine was predicted to induce a peak antibody titer in mice, SCTV01B induced a comparable IgG titer but a 3.7-fold higher NT₅₀ titer than RBD (Figure 3a,b). ELISpot results also showed that SCTV01B induced a higher frequency of splenic RBD-specific IFN- γ -SFCs than RBD (Figure 3c) and a similar frequency of splenic RBD-specific IL-4-SFCs as RBD (Figure 3d). As a result, the ratios of IFN- γ -SFCs to IL-4-SFCs in the SCTV01B group were higher than those in the RBD group (Figure 3e). Therefore, SCTV01B can induce more effective neutralizing antibodies and a Th1-biased cellular immune response profile in mice, demonstrating its significant advantages and desired features for an effective vaccine compared with the unconjugated RBD antigen, which induced a Th2-biased immune response.

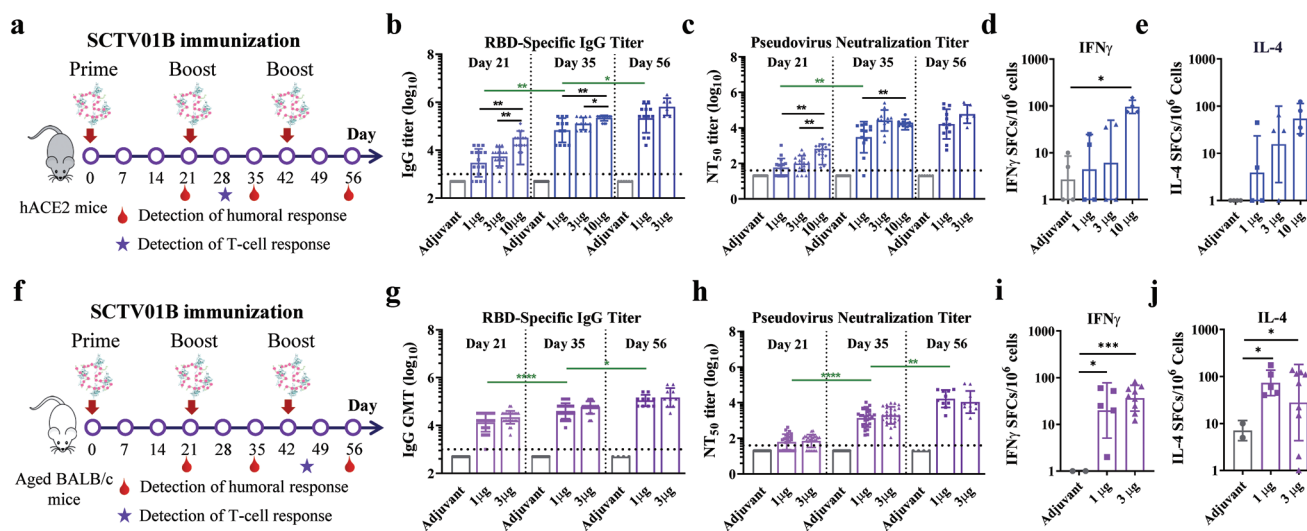


Figure 2. SCTV01B stimulates potent RBD-specific humoral and T-cell responses in both adult hACE2 mice and aged BALB/c mice. a,f). Schematic diagram of SCTV01B immunization and sample collection. Briefly, adult hACE2 mice and aged BALB/c mice were intramuscularly immunized with various doses of SCTV01B (1, 3, and 10 μg for hACE2 mice; 1 or 3 μg for aged BALB/c mice), and an equal volume of adjuvant alone was used as the negative control three times over an interval of 21 days. For detection of humoral response, tail vein blood samples were collected after each vaccination on schedule to prepare serum samples. The serum geometric mean RBD-specific antibody titer and NT₅₀ titer against the Wuhan-Hu-1 strain were determined by enzyme-linked immunosorbent assay (ELISA) and SARS-CoV-2 PSV neutralization assays at the indicated time points post-immunization, respectively. The dashed black lines indicate the limit of detection (LOD). The LOD of the RBD-specific antibody ELISA is 1000, and the LOD of the SARS-CoV-2 pseudovirus neutralization assay is 40. For detection of the T-cell response, mice were euthanized at 8 days for hACE2 mice or 25 days for aged BALB/c mice post first-boost immunization, and their spleens were dissected for enzyme-linked immunospot (ELISpot). b,c,g,h). RBD-specific IgG titer (b,g) and NT₅₀ titer (c,h) in sera of hACE2 mice ($n = 6\text{--}16$ per group) and aged BALB/c mice ($n = 4\text{--}27$ per group), respectively. Levels of RBD-specific IgG titers and NT₅₀ titers were compared across different dose groups of SCTV01B in hACE2 mice and in the 1 μg SCTV01B group after three injections in both hACE2 mice and aged BALB/c mice by unpaired two-tailed Welch's tests. * $p \leq 0.0186$, ** $p \leq 0.0064$, and *** $p < 0.0001$ represent statistical significance. The unlabeled comparisons were not significant, with $p \geq 0.0507$. d,e,i,j) The frequencies of RBD-specific IFN- γ SFCs (d,i) and IL-4 SFCs (e,j) in total splenocytes from hACE2 mice ($n = 4$ per group) and aged BALB/c mice ($n = 2\text{--}9$ per group) were determined by ELISpot. The adjuvant and different doses of SCTV01B were compared across groups by unpaired two-tailed Welch's tests. * $p \leq 0.0447$, *** $p = 0.0007$. The unlabeled comparisons were not significant, with $p \geq 0.0655$. Individual animal values are indicated by colored symbols.

2.4. SCTV01B Protected Mice from SARS-CoV-2 Challenge in Murine Models

To further explore the protective efficacy against SARS-CoV-2 in mice with prolonged time post-vaccination, hACE2 mice^[18] were intranasally challenged with 5.6×10^5 PFU of SARS-CoV-2 (BetaCoV/Beijing/IMEBJ05/2020) at 2 months after three doses of vaccination, and then viral load and histological changes in the lung tissues were determined at 5 or 7 days postinfection (dpi), respectively (Figure 4a). The results indicated that PBS-injected control mice showed high levels of viral RNAs (above 10^8 RNA copies g^{-1}) in the lung tissues at 5 and 7 dpi. As expected, immunization with 1 or 3 μg SCTV01B significantly decreased the virus load to the detection limit level, representing a reduction in the virus load of $>3.1 \log_{10}$ at 7 dpi (Figure 4b, Table S5, Supporting Information). More importantly, the histological results showed that immunization with 3 μg SCTV01B completely protected the mice from SARS-CoV-2-reducing lung damage, and immunization with 1 μg of SCTV01B significantly alleviated lung damage at 5 dpi with only mild lesions of alveolar epithelial cells, focal hemorrhage, and inflammatory cell infiltration (Figure 4c).

Aging is a significant risk factor for severe COVID-19 and death in humans.^[21] The protective effects of SCTV01B vaccination were also assessed in aged BALB/c mice with a lethal

mouse-adapted SARS-CoV-2 strain MASCP36.^[22] Following vaccination with 1 μg of SCTV01B or vehicle PBS alone twice for 1 month, mice were randomized and inoculated with 6×10^3 PFU of mouse-adapted SARS-CoV-2 MASCP36 (Figure 4d). Survival curve analysis showed that all mice in the PBS control group developed typical respiratory symptoms and eventually succumbed to severe acute respiratory disease syndrome (ARDS) within 5 days after MASCP36 challenge. Fortunately, all SCTV01B-vaccinated mice survived throughout the observation period (Figure 4e). Meanwhile, SCTV01B vaccination resulted in a ≈ 600 -fold reduction ($p < 0.01$) in viral RNA load compared with mice in the PBS control group at 3 dpi (Figure 4f). Histological examination revealed that lung tissues from the PBS control mice exhibited moderate to severe interstitial pneumonia, including increased thickness of the alveolar septum, inflammatory cell infiltration and congested blood vessels. The lung tissues from the SCTV01B-vaccinated mice displayed fewer lung lesions (Figure 4g).

2.5. SCTV01B Induced Potent Humoral and Balanced Th1/Th2 Cellular Immune Responses in Nonhuman Primates

To further explore the immunogenicity of SCTV01B in non-human primates, 10 μg of SCTV01B was administered to rhesus macaques for two doses at 21-day intervals. The results

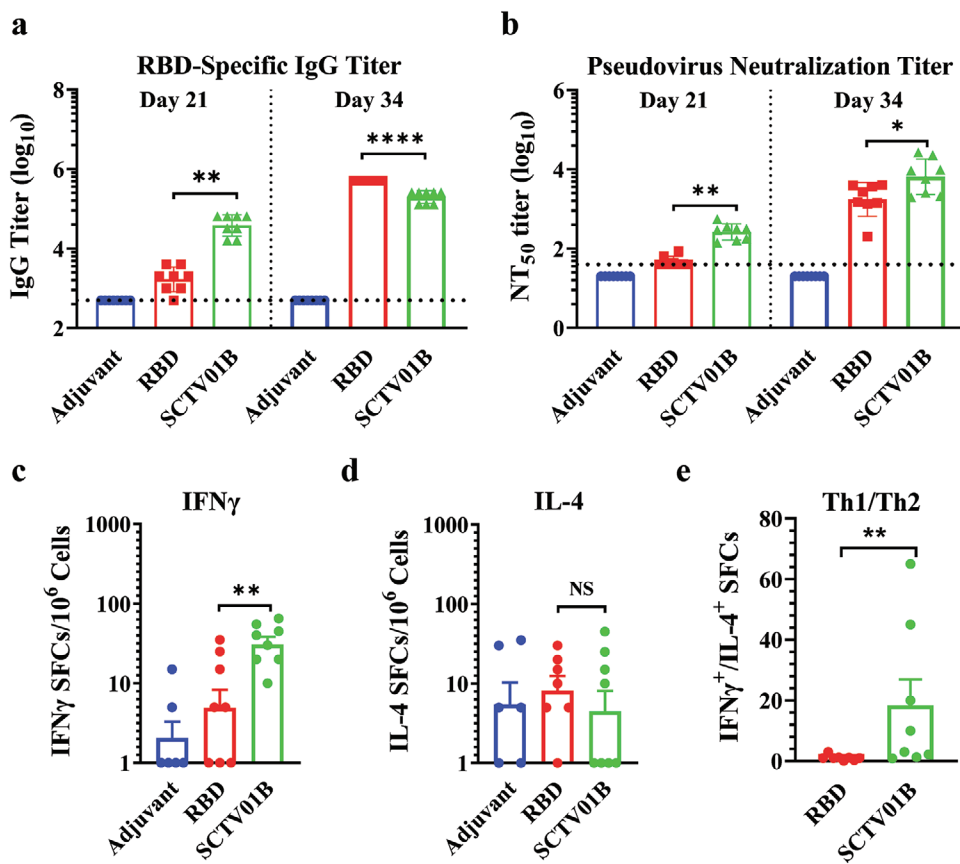


Figure 3. SCTV01B enhances RBD-specific immune responses in BALB/c mice. BALB/c mice ($n = 8$ per group) were immunized with 1 μg RBD or SCTV01B for two injections. a) Anti-RBD IgG titer was tested by ELISA. b) The NT₅₀ titer against the Wuhan-Hu-1 strain was analyzed by a SARS-CoV-2 PSV neutralization assay. The dashed black lines indicate the LOD. c) The numbers of RBD-specific IFN- γ SFCs and d) IL-4-SFCs in splenocytes were determined by ELISpot at 13 days postboosting. e) The ratios of IFN- γ SFCs to IL-4-SFCs were calculated. RBD and SCTV01B were compared by unpaired two-tailed Welch's tests. * $p = 0.0397$, ** $p \leq 0.0089$, and **** $p < 0.0001$. $p = 0.8121$ (NS) represented not significant. Individual animal values were indicated by colored symbols.

showed that SCTV01B vaccination induced high levels of anti-RBD IgG titers at 2 weeks post-prime immunization. The levels of the anti-RBD IgG titer peaked with 1/1149401 at day 14 post-boosting, with a 29-fold increase compared with the peak titer after prime vaccination (Figure 5a). A more obvious increase of 177-fold in the peak NT₅₀ titer after boost dose was observed in the SCTV01B-vaccinated rhesus macaques (Figure 5b). RBD-specific IFN- γ SFCs and IL-4-SFCs were significantly increased at 7 days postboosting, and a high ratio of IFN- γ SFCs and IL-4-SFCs was observed in the SCTV01B-vaccinated group (Figure 5c–e). Additionally, serum samples from rhesus macaques vaccinated with SCTV01B at 21 days after boosting vaccination were tested for NT₅₀ titer against the pseudoviruses of the original Wuhan-Hu-1, D614G strain (B.1); VOCs: Alpha (B.1.1.7), Beta (B.1.351), Gamma (P.1), Delta (B.1.617.2), and its subtypes AY.1, AY.2, and AY.3, and Omicron (B.1.1.529); variants of interest (VOIs): Lambda (C.37), Mu (B.1.621); variants under monitoring (VUMs): Epsilon (B.1.427, B.1.429), Iota (B.1.526), and Kappa (B.1.617.1); and other variants such as B.1.618 strains. The results demonstrated that SCTV01B induced a broad spectrum of neutralizing antibodies against SARS-CoV-2 variants due to sequence conservation, as the neutralization titers were similar against both the original D614G and Wuhan-Hu-1

strains, moderately decreased against the Alpha, Delta, Lambda, and Epsilon variants, and 7–25-fold decreased against the Beta, Gamma, Mu, Iota, Kappa, and Omicron variants with the E484 substitution (Figure 5f; Table S6, Supporting Information).

2.6. SCTV01B Immunization Induced a Protective Immune Response to PPS14 in Rhesus Macaques

Because our nanoparticle vaccine SCTV01B contained both RBD and PPS14 as immunogens, we further sought to determine whether protective immunity against *S. pneumoniae* was induced. Serum samples from SCTV01B-immunized rhesus monkeys were tested. As expected, the background anti-PPS14 antibody titer was low but increased dramatically and reached $>10^4$ after two injections of SCTV01B (Figure 6a). The serum also showed high opsonophagocytic activity (OPA) against *S. pneumoniae* serotype 14 compared with that of the adjuvant control (Figure 6b,c). A previous study has indicated that the level of OPA portended good protective efficacy in monkey models.^[23] These results indicated that in addition to prevention of COVID-19, SCTV01B would probably have the added potential benefit of prophylaxis against *S. pneumoniae* serotype 14-related pneumococcal disease.

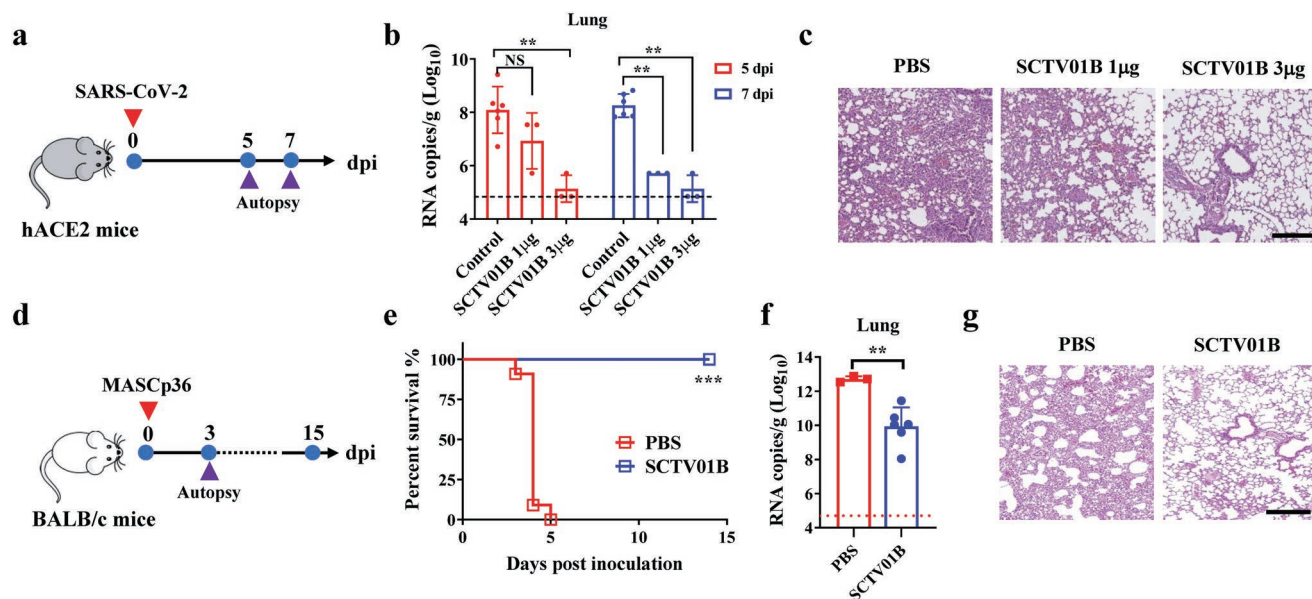


Figure 4. Protective efficacy of SCTV01B in hACE2 mice and aged BALB/c mice. a,d) Schematic diagram of the protective experiment in hACE2 mice and aged BALB/c mice. b) The viral load in the lungs of hACE2 mice at 5 and 7 dpi was analyzed in the indicated groups ($n = 6$ in the PBS group and $n = 3$ in the vaccinated groups). Comparisons were performed by two-tailed Mann–Whitney tests. $**p \leq 0.0013$. $p = 0.1840$ (NS) represents not significant. The dashed line indicates the LOD of $4.8 \log_{10}$ RNA copies g^{-1} . c) Representative histopathology in the lungs of SCTV01B- and PBS-vaccinated hACE2 mice after challenge with SARS-CoV-2 at 5 dpi. e) Percentage survival of aged BALB/c mice after vaccination with SCTV01B and PBS control ($n = 6$ per group). Comparisons were performed by two-tailed Mann–Whitney tests. $***p = 0.0002$. f) The viral load in the lungs of aged BALB/c mice at 3 dpi. Comparisons were performed by two-tailed Mann–Whitney tests. $**p = 0.0015$. The dashed line indicates the LOD of $4.8 \log_{10}$ RNA copies g^{-1} . g) Representative histopathology in the lungs of SCTV01B- and PBS-vaccinated aged BALB/c mice after challenge with SARS-CoV-2. Scale bar: 200 μm . Individual animal values are indicated by colored symbols.

3. Discussion

This study reports a novel COVID-19 vaccine candidate composed of nanoparticles of PPS14-conjugated RBD protein and squalene-based emulsion adjuvant. Our results indicated that the conjugation of RBD proteins with PPS14 polysaccharides and the formation of nanoparticles led to significantly enhanced immunogenicity compared with unconjugated RBD protein. Two injections of SCTV01B with adjuvant enhanced antigen presentation and recruitment of immune cells^[24] and induced potent RBD-specific humoral responses and balanced Th1 and Th2 immunity in animal models, including aged BALB/c mice and rhesus macaques. High neutralizing antibody titers with sustained Th1 responses were considered to correlate with protection against viral replication.^[25] Th1-biased immune responses have favorable antiviral properties, whereas Th2-biased responses have been associated with vaccine-associated enhanced respiratory disease (VAERD).^[26] Thus, the immune profile induced by SCTV01B in mice indicated a low risk of vaccine-enhanced disease upon SARS-CoV-2 challenge.

SCTV01B exhibited broad-spectrum and high neutralizing antibody titers against various SARS-CoV-2 variants, especially the VOCs (B.1.617.2 and its subtype AY.1, AY.2, AY.3, and B.1.1.7, B.1.351), but reduced titers against P.1, B.1.1.529, B.1.621, and B.1.526 with E484 substitution. An obvious decrease in neutralization titers against the Beta variant was also reported in humans who were injected with the original strain SARS-CoV-2 vaccines, such as BNT162b2,^[27] ChAdOx1,^[27] and Ad26.COV2. S,^[27–28] mRNA-1273,^[29] NVX-CoV2373,^[29b] and ZF2001.^[30] In addition,

a remarkable decline in neutralization against the Omicron variant by sera from COVID-19 vaccine recipients was verified.^[31,32] Therefore, a third boosting dose or new vaccine based on variants is needed to further improve the spectrum of neutralization against pandemic variants and enhance its antiviral effect.

Improvements in viral load and pathology in the lungs of a nonlethal hACE2 mouse model are key indexes for evaluating the protective efficacy of NVX-CoV2373.^[33] SCTV01B vaccination demonstrated clear protective efficacy in a published nonlethal hACE2 virus challenge mouse model^[22] using common assessment protocols. More importantly, it significantly protected aged mice from SARS-CoV-2 infection-induced pneumonitis, lung damage, and death. These data suggest that this novel vaccine may be a promising vaccine candidate for the prevention of SARS-CoV-2 infection-induced COVID-19 in humans, especially elderly people.

PPS14, as a component of SCTV01B, was used to increase the diameter of RBD antigen nanoparticles to dozens of nanometers and target the antigen to DC cells by binding to sugar receptors expressed on DC cells, which enhanced vaccine internalization, phagocytosis, and presentation by antigen-presenting cells such as macrophages and DCs.^[16a,b] We found that vaccination with the same dose of SCTV01B induced more potent humoral and cellular immune responses than vaccination with recombinant RBD (Figure 3). Interestingly, vaccination with SCTV01B also induced potent anti-PPS14 antibodies with high OPA in rhesus monkeys (Figure 6). In some animal and clinical studies, the OPA levels have been well demonstrated as a better surrogate

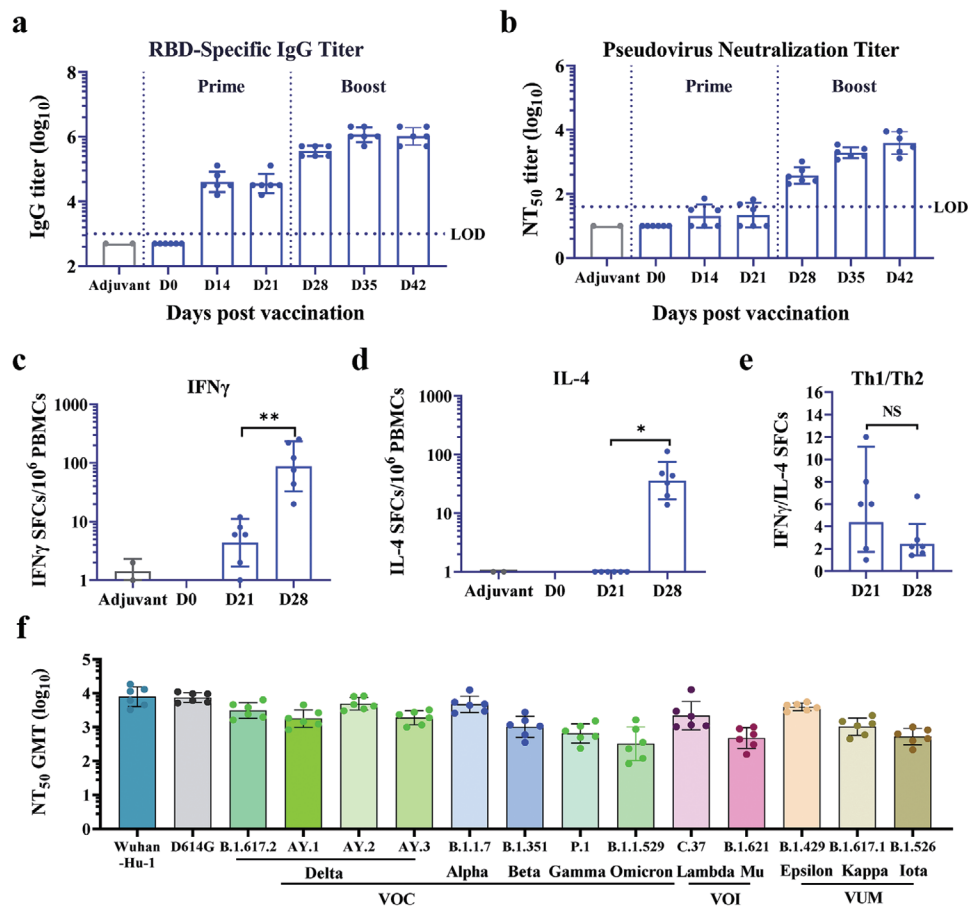


Figure 5. SCTV01B stimulates potent RBD-specific immune responses in rhesus macaques. Rhesus macaques were immunized with adjuvant alone ($n = 2$) or $10 \mu\text{g}$ SCTV01B ($n = 6$) for two injections. a) The RBD-specific IgG titer measured by ELISA. b) NT_{50} titer against the Wuhan-1 strain detected by the SARS-CoV-2 PSV neutralization assay. The dashed line indicates the LOD. c) The frequency of $\text{IFN-}\gamma$ -SFCs and d) IL-4-SFCs in PBMCs was determined by ELISpot. e) The ratios of $\text{IFN-}\gamma$ to IL-4-SFCs were calculated. Comparisons were made between the prime (D21) and boost (D28) injections of SCTV01B and performed by two-tailed Welch's tests. $*p = 0.0293$, $**p = 0.0022$. $p = 0.1412$ (NS) represents not significant. f) Broad-spectrum neutralization activities against SARS-CoV-2 Wuhan-Hu-1, D614G, VOCs (Alpha, Beta, Gamma, Delta, and the Omicron subvariants), VOIs (Mu and Lambda), and VUMs (Epsilon, Kappa, and Iota) were measured by PSV neutralization assay. Individual animal values are indicated by colored symbols.

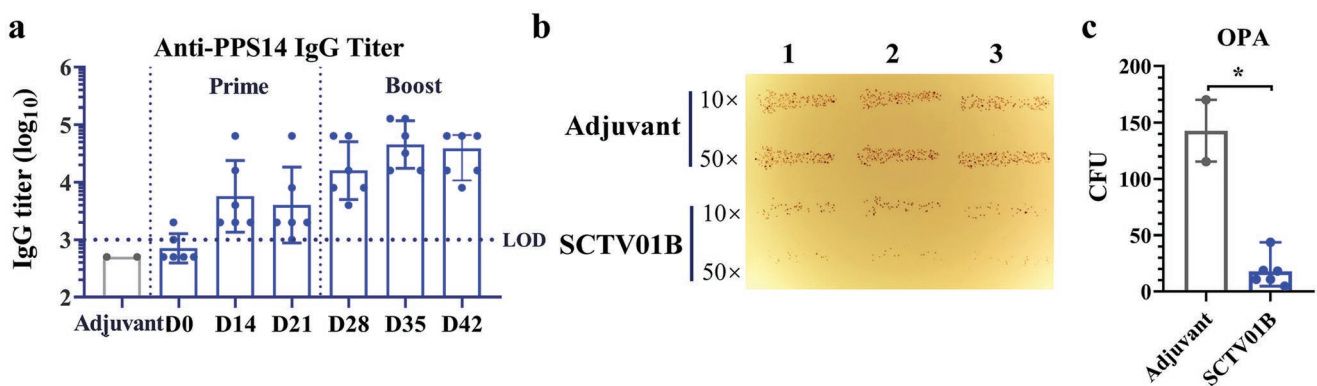


Figure 6. SCTV01B stimulates anti-PPS14-specific antibody responses in rhesus macaques. Rhesus macaques ($n = 6$) were immunized with $10 \mu\text{g}$ SCTV01B for two injections. a) The anti-PPS14-specific IgG titer measured by ELISA. The dashed line indicates the LOD. b) Representative photo of *S. pneumoniae* serotype 14-specific opsonophagocytic assay in $10\times$ or $50\times$ SCTV01B-immunized serum. Each dilution had three duplicates. c) OPA in $50\times$ dilutions of SCTV01B-immunized sera ($n = 6$) determined by opsonophagocytic assay. The SCTV01B and adjuvant groups were compared by two-tailed Mann-Whitney tests. $*p = 0.0357$. Individual animal values are indicated by colored symbols.

marker of vaccine efficacy than IgG titers.^[34] For example, a minimum OPA titer with one-eighth conferred protection in a mouse model and was correlated with protection in infants vaccinated with pneumococcal conjugate vaccine.^[34b] Similarly, the OPA titers measured from sera of human infants vaccinated with PCV15 also showed a good correlation with that observed in infant rhesus macaques. In contrast, there was no correlation in serum IgG levels between human infants and animal models.^[23] Additionally, passive protective efficacy was also observed in an *S. pneumoniae* mouse challenge model by administering human serum with high OPA titers.^[35] Thus, immunization with SCTV01B was supposed to confer a full protection against *S. pneumoniae* infection.

The adjuvant used in SCTV01B is an oil-in-water emulsion adjuvant containing squalene, which can enhance both humoral and cellular immune responses and improve the overall protective efficacy of vaccines.^[36] This type of adjuvant was reported to enhance the immunogenicity of the Hib-polysaccharide conjugate vaccine^[37] and was used in the influenza vaccine FLUAD to generate a strong immune response in elderly adults above 65 years old for prophylaxis of the flu. Both the long durability of responses and the increase in CD154-expressing CD4⁺ T and CD8⁺ T cells, which indicated robust memory B-cell responses, were observed in SCTV01B-immunized mice by using this type of adjuvant (Figures S2 and S4, Supporting Information). Therefore, SCTV01B can be a promising vaccine candidate for COVID-19, and the strategy of polysaccharide-conjugated protein-based vaccines could be of value in fighting infectious diseases.

4. Experimental Section

All experiments with live SARS-CoV-2 were performed in biosafety level 3 (BSL3) facilities and approved by the Animal Experiment Committee of Laboratory Animal Center, Beijing Institute of Microbiology and Epidemiology (approval number: IACUC-DWZX-2020-002). All animal experiments were conducted according to the Chinese animal use guidelines and were approved by the Institutional Animal Care and Use Committee (IACUC) (approval number: ACU21-929).

Statistical Analysis: Serum anti-RBD titer, NAT₅₀ titer, and anti-PPS14 titer were plotted with individual values and presented as geometric mean \pm SD. RBD-specific T cells of IFN- γ , IL-4, or CD154, viral load of lung tissues, and OPA activity of serum were plotted with individual values and presented as arithmetic means \pm SD. Comparisons among groups were conducted by unpaired, two-tailed *t*-test with Welch's tests in immunogenicity study or Mann-Whitney tests in virus challenging study using GraphPad Prism 8. *p*-Value of * <0.05 , ** <0.01 , *** <0.001 , and **** <0.0001 were considered statistically significant.

Details of the reagents and experimental methods used can be found in the Supporting Information.

Supporting Information

Supporting Information is available from the Wiley Online Library or from the author.

Acknowledgements

This work was supported by the Beijing Municipal Science and Technology Program (Z211100002521026) and the National Natural

Science Foundation of China (NSFC) (32130005, and 82174055). C.Q. was supported by the National Science Fund for Distinguished Young Scholars (81925025), the Innovative Research Group (81621005) from the NSFC, and the Innovation Fund for Medical Sciences (2019-I2M-5-049) from the Chinese Academy of Medical Sciences.

Conflict of Interest

The authors declare no conflict of interest.

Author Contributions

Y.D., J.L., C.S., and H.C. contributed equally to this work. J.L., C.S., R.W., Y.D., C.Q., and X.Z. wrote the manuscript. C.S. designed the vaccine antigens. J.L., C.S., R.W., X.Z., Y.D., and Y.Z. designed the experiments. R.W. and X.Z. conducted the in vivo immunization studies. Y.D., H.C., D.L., H.Q., M.W., and X.H. performed the animal experiments and analyzed the data. Y.Z. provided materials (protein expression and purification, squalene-based emulsion adjuvant and polysaccharide manufacture, and chemical coupling of the conjugated nanoparticle). C.Q. and L.X. supervised the study and finalized the manuscript. All authors discussed the results and commented on the manuscript.

Data Availability Statement

The data that support the findings of this study are available on request from the corresponding author. The data are not publicly available due to privacy or ethical restrictions.

Keywords

capsular polysaccharide, chemical conjugation, receptor binding domain, nanoparticle vaccines, SARS-CoV-2, *S. pneumoniae* serotype type 14

Received: January 14, 2022

Revised: March 18, 2022

Published online: April 21, 2022

[1] a) H. Wang, Y. Zhang, B. Huang, W. Deng, Y. Quan, W. Wang, W. Xu, Y. Zhao, N. Li, J. Zhang, H. Liang, L. Bao, Y. Xu, L. Ding, W. Zhou, H. Gao, J. Liu, P. Niu, L. Zhao, W. Zhen, H. Fu, S. Yu, Z. Zhang, G. Xu, C. Li, Z. Lou, M. Xu, C. Qin, G. Wu, G. F. Gao, et al., *Cell* **2020**, *182*, 713; b) S. Xia, Y. Zhang, Y. Wang, H. Wang, Y. Yang, G. F. Gao, W. Tan, G. Wu, M. Xu, Z. Lou, W. Huang, W. Xu, B. Huang, H. Wang, W. Wang, W. Zhang, N. Li, Z. Xie, L. Ding, W. You, Y. Zhao, X. Yang, Y. Liu, Q. Wang, L. Huang, Y. Yang, G. Xu, B. Luo, W. Wang, P. Liu, et al., *Lancet Infect. Dis.* **2021**, *21*, 39.

[2] N. van Doremalen, T. Lambe, **2020**, *586*, 578.

[3] a) K. Wu, A. P. Werner, M. Koch, A. Choi, E. Narayanan, G. B. E. Stewart-Jones, T. Colpitts, H. Bennett, S. Boyoglu-Barnum, W. Shi, J. I. Moliva, N. J. Sullivan, B. S. Graham, A. Carfi, K. S. Corbett, R. A. Seder, D. K. Edwards, *N. Engl. J. Med.* **2021**, *384*, 1468; b) K. S. Corbett, D. K. Edwards, S. R. Leist, O. M. Abiona, S. Boyoglu-Barnum, R. A. Gillespie, S. Himansu, A. Schäfer, C. T. Ziwawo, A. T. DiPiazza, K. H. Dinno, S. M. Elbashir, C. A. Shaw, A. Woods, E. J. Fritch, D. R. Martinez, K. W. Bock, M. Minai, B. M. Nagata, G. B. Hutchinson, K. Wu, C. Henry, K. Bahl,

- D. Garcia-Dominguez, L. Ma, I. Renzi, W. P. Kong, S. D. Schmidt, L. Wang, Y. Zhang, et al., *Nature* **2020**, 586, 567.
- [4] a) J.-H. Tian, N. Patel, R. Haupt, H. Zhou, S. Weston, H. Hammond, J. Logue, A. D. Portnoff, J. Norton, M. Guebre-Xabier, B. Zhou, K. Jacobson, S. Maciejewski, R. Khatoun, M. Wisniewska, W. Moffitt, S. Kluepfel-Stahl, B. Ekechukwu, J. Papin, S. Boddapati, C. Jason Wong, P. A. Piedra, M. B. Frieman, M. J. Massare, L. Fries, K. L. Bengtsson, L. Stertman, L. Ellingsworth, G. Glenn, G. Smith, *Nat. Commun.* **2021**, 12, 372; b) C. Keech, G. Albert, I. Cho, A. Robertson, P. Reed, S. Neal, J. S. Plested, M. Zhu, S. Cloney-Clark, H. Zhou, G. Smith, N. Patel, M. B. Frieman, R. E. Haupt, J. Logue, M. McGrath, S. Weston, P. A. Piedra, C. Desai, K. Callahan, M. Lewis, P. Price-Abbott, N. Formica, V. Shinde, L. Fries, J. D. Lickliter, P. Griffin, B. Wilkinson, G. M. Glenn, *N. Engl. J. Med.* **2020**, 383, 2320.
- [5] W. Tai, L. He, X. Zhang, J. Pu, D. Voronin, S. Jiang, Y. Zhou, L. Du, *Cell Mol. Immunol.* **2020**, 17, 613.
- [6] K. K. To, O. T. Tsang, W. S. Leung, A. R. Tam, T. C. Wu, D. C. Lung, C. C. Yip, J. P. Cai, J. M. Chan, T. S. Chik, D. P. Lau, C. Y. Choi, L. L. Chen, W. M. Chan, K. H. Chan, J. D. Ip, A. C. Ng, R. W. Poon, C. T. Luo, V. C. Cheng, J. F. Chan, I. F. Hung, Z. Chen, H. Chen, K. Y. Yuen, *Lancet Infect. Dis.* **2020**, 20, 565.
- [7] L. Dai, T. Zheng, K. Xu, Y. Han, L. Xu, E. Huang, Y. An, Y. Cheng, S. Li, M. Liu, M. Yang, Y. Li, H. Cheng, Y. Yuan, W. Zhang, C. Ke, G. Wong, J. Qi, C. Qin, J. Yan, G. F. Gao, *Cell* **2020**, 182, 722.
- [8] a) T. K. Tan, P. Rijal, R. Rahikainen, A. H. Keeble **2021**, 12, 542; b) L. Zha, X. Chang, H. Zhao, M. O. Mohsen, *Vaccines (Basel)* **2021**, 9, 395; c) C. Fougeroux, L. Goksoyr, M. Idorn, V. Soroka, S. K. Myeni, R. Dagil, C. M. Janitzek, M. Søgaard, K.-L. Aves, E. W. Horsted, S. M. Erdoğan, T. Gustavsson, J. Dorosz, S. Clemmensen, L. Fredsgaard, S. Thrane, E. E. Vidal-Calvo, P. Khalifé, T. M. Hulen, S. Choudhary, M. Theisen, S. K. Singh, A. Garcia-Senosiani, L. von Oosten, G. Pijlman, B. Hierzberger, T. Domeyer, B. W. Nalewajek, A. Strøbæk, M. Skrzypczak, *Nat. Commun.* **2021**, 12, 324.
- [9] a) W. C. Huang, S. Zhou, X. He, K. Chiem, M. T. Mabrouk, R. H. Nissly, I. M. Bird, M. Strauss, S. Sambhara, J. Ortega, E. A. Wohlfert, L. Martinez-Sobrido, S. V. Kuchipudi, B. A. Davidson, J. F. Lovell, *Adv. Mater.* **2020**, 32, 2005637; b) K. S. Park, J. D. Bazzill, S. Son, J. Nam, S. W. Shin, L. J. Ochyl, J. A. Stuckey, J. L. Meagher, L. Chang, J. Song, D. C. Montefiori, C. C. LaBranche, J. L. Smith, J. Xu, J. J. Moon, *J. Controlled Release* **2021**, 330, 529.
- [10] U. Kalathiya, M. Padariya, R. Fahraeus, S. Chakraborti, T. R. Hupp, *Biomolecules* **2021**, 11, 297.
- [11] L. Li, M. Wang, J. Hao, J. Han, T. Fu, J. Bai, M. Tian, N. Jin, G. Zhu, C. Li, *Int. J. Biol. Macromol.* **2021**, 190, 409.
- [12] T. Gao, Y. Ren, S. Li, X. Lu, H. Lei, **2021**, 20, 95.
- [13] a) J. Eskola, A. K. Takala, H. Käyhty, *Curr. Opin. Pediatr.* **1993**, 5, 55; b) G. A. Poland, *Clin. Infect. Dis.* **2010**, 50, S45; c) M. Nair, *Indian J. Community Med.* **2012**, 37, 79.
- [14] M. E. Pichichero, *Hum. Vaccines Immunother.* **2013**, 9, 2505.
- [15] T. G. Dacoba, R. W. Omange, H. Li, J. Crecente-Campo, M. Luo, M. J. Alonso, *ACS Nano* **2019**, 13, 4947.
- [16] a) S. Zamze, L. Martinez-Pomares, H. Jones, P. R. Taylor, R. J. Stillion, S. Gordon, S. Y. Wong, *J. Biol. Chem.* **2002**, 277, 41613; b) E. W. Adams, D. M. Ratner, P. H. Seeberger, N. Hacohen, *Chem-BioChem* **2008**, 9, 294; c) U. Meltzer, D. Goldblatt, *Infect. Immun.* **2006**, 74, 1890.
- [17] A. Weintraub, *Carbohydr. Res.* **2003**, 338, 2539.
- [18] S. H. Sun, Q. Chen, H. J. Gu, G. Yang, Y. X. Wang, X. Y. Huang, S. S. Liu, N. N. Zhang, X. F. Li, R. Xiong, Y. Guo, Y. Q. Deng, W. J. Huang, Q. Liu, Q. M. Liu, Y. L. Shen, Y. Zhou, X. Yang, T. Y. Zhao, C. F. Fan, Y. S. Zhou, C. F. Qin, Y. C. Wang, *Cell Host Microbe* **2020**, 28, 124.
- [19] H. Gu, Q. Chen, G. Yang, L. He, H. Fan, Y. Q. Deng, Y. Wang, Y. Teng, Z. Zhao, Y. Cui, Y. Li, X. F. Li, J. Li, N. N. Zhang, X. Yang, S. Chen, Y. Guo, G. Zhao, X. Wang, D. Y. Luo, H. Wang, X. Yang, Y. Li, G. Han, Y. He, X. Zhou, S. Geng, X. Sheng, S. Jiang, S. Sun, et al., *Science* **2020**, 369, 1603.
- [20] E. J. Anderson, N. G. Roupael, A. T. Widge, L. A. Jackson, P. C. Roberts, M. Makhene, J. D. Chappell, M. R. Denison, L. J. Stevens, A. J. Pruijssers, A. B. McDermott, B. Flach, B. C. Lin, N. A. Doria-Rose, S. O'Dell, S. D. Schmidt, K. S. Corbett, P. A. Swanson, M. Padilla, K. M. Neuzil, H. Bennett, B. Leav, M. Makowski, J. Albert, K. Cross, V. V. Edara, K. Floyd, M. S. Suthar, D. R. Martinez, et al., *N. Engl. J. Med.* **2020**, 383, 2427.
- [21] E. E. Walsh, R. W. Frenck, A. R. Falsey, N. Kitchin, J. Absalon, A. Gurtman, S. Lockhart, K. Neuzil, M. J. Mulligan, R. Bailey, K. A. Swanson, P. Li, K. Koury, W. Kalina, D. Cooper, C. Fontes-Garfias, P.-Y. Shi, Ö. Türeci, K. R. Tompkins, K. E. Lyke, V. Raabe, P. R. Dormitzer, K. U. Jansen, U. Şahin, W. C. Gruber, *N. Engl. J. Med.* **2020**, 383, 2439.
- [22] S. Sun, H. Gu, L. Cao, Q. Chen, Q. Ye, G. Yang, R. T. Li, H. Fan, *Nat. Commun.* **2021**, 12, 5654.
- [23] J. Xie, Y. Zhang, I. Caro-Aguilar, L. Indrawati, W. J. Smith, C. Giovarelli, M. A. Winters, J. MacNair, J. He, C. Abeygunawardana, L. Musey, M. Kosinski, J. M. Skinner, *Pediatr. Infect. Dis. J.* **2020**, 39, 70.
- [24] A. Seubert, E. Monaci, M. Pizza, D. T. O'Hagan, A. Wack, *J. Immunol.* **2008**, 180, 5402.
- [25] Y. Sui, Y. Bekele, J. A. Berzofsky, *Pathogens (Basel, Switzerland)* **2021**, 10, 138.
- [26] B. S. Graham, *Science* **2020**, 368, 945.
- [27] C. Liu, H. M. Ginn, W. Dejnirattisai, P. Supasa, B. Wang, A. Tuekprakhon, R. Nutalai, D. Zhou, A. J. Mentzer, Y. Zhao, H. M. E. Duyvesteyn, C. López-Camacho, J. Slon-Campos, T. S. Walter, D. Skelly, S. A. Johnson, T. G. Ritter, C. Mason, S. A. Costa Clemens, F. Gomes Naveca, V. Nascimento, F. Nascimento, C. Fernandes da Costa, P. C. Resende, A. Pauvolid-Correa, M. M. Siqueira, C. Dold, N. Temperton, T. Dong, A. J. Pollard, et al., *Cell* **2021**, 184, 4220.
- [28] M. Jongeneelen, K. Kaszas, D. Veldman, J. Huizingh, R. van der Vlugt, T. Schouten, D. Zuijdgeest, T. Uil, G. van Roey, N. Guimera, M. Navis, R. Bos, M. le Gars, J. Sadoff, L. Muchene, J. Juraszek, J. P. M. Langedijk, R. Vogels, J. Custers, H. Schuitemaker, B. Brandenburg, *bioRxiv* **2021**, <https://doi.org/10.1101/2021.07.01.450707>.
- [29] a) A. Choi, M. Koch, K. Wu, G. Dixon, J. Oestreicher, H. Legault, G. B. E. Stewart-Jones, T. Colpitts, R. Pajon, H. Bennett, A. Carfi, D. K. Edwards, *J. Virol.* **2021**, 95, e0131321; b) X. Shen, H. Tang, R. Pajon, G. Smith, G. M. Glenn, W. Shi, B. Korber, D. C. Montefiori, *N. Engl. J. Med.* **2021**, 384, 2352.
- [30] X. Zhao, A. Zheng, D. Li, R. Zhang, H. Sun, Q. Wang, G. F. Gao, P. Han, L. Dai, *bioRxiv* **2021**, <https://doi.org/10.1101/2021.07.15.452504>.
- [31] W. Dejnirattisai, R. H. Shaw, P. Supasa, C. Liu, A. S. V. Stuart, A. J. Pollard, X. Liu, T. Lambe, D. Crook, D. I. Stuart, J. Mongkolsapaya, J. S. Nguyen-Van-Tam, M. D. Snape, G. R. Screaton, *Lancet* **2022**, 399, 234; b) A. Wilhelm, M. Widera, K. Grikscheit, T. Toptan, B. Schenk, C. Pallas, M. Metzler, N. Kohmer, S. Hoehl, F. A. Helfritz, T. Wolf, U. Goetsch, S. Ciesek, *medRxiv* **2021**, <https://doi.org/10.1101/2021.12.07.21267432>; c) A. Rössler, L. Riepler, D. Bante, D. von Laer, J. Kimpel, *N. Engl. J. Med.* **2022**, 386, 698.
- [32] a) S. Cele, L. Jackson, D. S. Khoury, K. Khan, T. Moyo-Gwete, H. Tegally, J. E. San, D. Cromer, C. Scheepers, D. G. Amoako, F. Karim, M. Bernstein, G. Lustig, D. Archary, M. Smith, D. Cromer, Y. Ganga, J. Zesuliwe, K. Reedy, S. H. Hwa, J. Giandhari, J. M. Blackburn, B. I. Gosnell, S. S. von Abdool Karim, W. Hanekom, A. von Gottberg, J. N. Bhiman, R. J. Lessells, M. S. de Moosa, M. P. Davenport, NGS-SA, COMMIT-KZN Team, et al., *Nature*

- 2022, 602, 654; b) F. Schmidt, F. Muecksch, Y. Weisblum, J. Da Silva, E. Bednarski, A. Cho, Z. Wang, C. Gaebler, M. Caskey, M. C. Nussenzweig, T. Hatziioannou, P. D. Bieniasz, *N. Engl. J. Med.* **2022**, 386, 599.
- [33] J. H. Tian, N. Patel, R. Haupt, H. Zhou, S. Weston, **2021**, 12, 372.
- [34] a) S. Romero-Steiner, C. E. Frasch, G. Carlone, R. A. Fleck, D. Goldblatt, M. H. Nahm, *Clin. Vaccine Immunol.* **2006**, 13, 165; b) L. Jódar, J. Butler, G. Carlone, R. Dagan, D. Goldblatt, H. Käyhty, K. Klugman, B. Plikaytis, G. Siber, R. Kohberger, I. Chang, T. Cherian, *Vaccine* **2003**, 21, 3265; c) J. Y. Song, M. A. Moseley, R. L. Burton, M. H. Nahm, *J Infect Chemother* **2013**, 19, 412.
- [35] S. E. Johnson, L. Rubin, S. Romero-Steiner, J. K. Dykes, L. B. Pais, A. Rizvi, E. Ades, G. M. Carlone, *J. Infect. Dis.* **1999**, 180, 133.
- [36] a) E.-J. Ko, S.-M. Kang, *Hum. Vaccines Immunother.* **2018**, 14, 3041; b) E. S. Bergmann-Leitner, W. W. Leitner, *Vaccines (Basel)* **2014**, 2, 252; c) J. G. Liang, D. Su, T.-Z. Song, Y. Zeng, W. Huang, J. Wu, R. Xu, P. Luo, X. Yang, X. Zhang, S. Luo, Y. Liang, X. Li, J. Huang, Q. Wang, X. Huang, Q. Xu, M. Luo, A. Huang, D. Luo, C. Zhao, F. Yang, J.-B. Han, Y.-T. Zheng, P. Liang, *Nat. Commun.* **2021**, 12, 1346.
- [37] D. M. Granoff, Y. E. McHugh, H. V. Raff, A. S. Mokatri, G. A. Van Nest, *Infect. Immun.* **1997**, 65, 1710.